European Journal of Soil Science, doi: 10.1111/ejss.12407 (2017)

Reducing conditions in soil of Gallocanta Lake, NE Spain

C. CASTAÑEDA[a], E. LUNA[a] & M. RABENHORST[b]

[a] *Estación Experimental de Aula Dei, EEAD-CSIC, Ave. Montañana 1005, 50059 Zaragoza, Spain,* [b] *Department of Environmental Science and Technology, University of Maryland, 1109 HJ Patterson Hall, College Park, MD 20740, USA*

Correspondence: C. Castañeda. E-mail: ccastaneda@eead.csic.es

Short title: Reducing conditions in soil

Summary

Saline wetlands have received limited attention only from researchers, and this neglect has often resulted in their degradation, limited conservation, and insufficient information to design conservation and management plans. Gallocanta Lake is a Natural Reserve of international importance for winter birds although soil resources, which support of endemisms and protected habitats, have been recognized more recently. The soil of Gallocanta Lake undergoes strong oscillations of saturation and drainage followed by drying because of irregular rain and variable flooding conditions associated with fluctuations in the level of the lake. This study examined reducing conditions and morphological indicators of reduction of soils around the lake with indicators of reduction in soils (IRIS) tubes, which are coated with iron oxides. We surveyed five sites for between 22 and 34 weeks. The average amount of iron removed from the IRIS tubes during the period studied ranged between 4 and 96%. The intensity of reduction in the soil differs according to subtle topographic differences between sites; it increases with the decrease in elevation. The large soil salinity (ECe from 18.1 to 182 dS m^{-1}), carbonate-rich composition (from 18.4 to 69.7% CCE) and overall small organic matter content (from 0.4 to 6.2% OM) do not seem to constrain iron mobilization because of the reducing conditions. Differences in iron depletion and patterns on the IRIS tubes show the heterogeneity of soil conditions and the complexity of factors involved in redox processes. Further research is needed to gain knowledge of the redox processes in the context of pedogenesis in semiarid lacustrine environments.

Keywords: hydromorphic soils, indicator of reduction in soils (IRIS) tubes, lacustrine, semiarid, soil micromorphology, soil reduction, soil salinity

Highlights:

- **How intermittently exposed soils are expressing the redox conditions?**
- **Current reducing conditions are evidenced in a fluctuating saline lake by IRIS tubes**
- **Soil reduction occurs in alkaline soils with intermittent waterlogging**
- **IRIS tubes are suitable field indicators of soil reducing conditions heterogeneity in saline lakes**

Introduction

Most recent studies of water levels of the Gallocanta Lake have focused on the effects of climatic and hydrological changes (Comín *et al*., 1983; Rodó *et al*., 2002). Few studies have focused on morphological changes in saline soil of shallow fluctuating lakes, where pedogenesis is strongly related to the water level of the lake. The intermittent desiccation of Gallocanta lake, especially during the last few decades because of the decrease of rainfall (Luna *et al*., 2016), has favoured the succession of subaqueous and oxidizing conditions in the soil that leads to variable saturation. Redoximorphic features in Gallocanta Lake have been described recently in lakebed sediments and soil, and also in the peripheral agricultural soil (Castañeda *et al*., 2015).

Reducing soil conditions related to anaerobic conditions have agronomic, ecologic and environmental significance, and their importance to wetland functions is widely recognized (Craft, 2001). The reducing conditions in soil are of interest for delineating wetland soil or to confirm the hydric conditions of soil for regulatory purposes (Rabenhorst, 2008). The occurrence of redoximorphic features is a key in many international soil classification systems to infer reducing conditions in soil (reviewed by Dorau & Mansfeldt, 2015). A field method for identifying reducing conditions in soil

63 based on the indicator of reduction in soils (IRIS) tubes was developed by Jenkinson &
64 Franzmeier (2006), adapted by Rabenhorst & Burch (2006) and evaluated in floodplain
65 areas by Castenson & Rabenhorst (2006). This field method has been approved by the
66 National Technical Committee for Hydric Soils (NTCHS) as a standard method and
67 field indicator of reduced soil conditions in the USA (Rabenhorst, 2012) in wetland
68 delineations. The IRIS tubes have been used for to document reducing conditions in
69 wetland soil (Rabenhorst, 2008; Dorau & Mansfeldt, 2015; Dorau *et al*., 2016) and, less
70 frequently, in agricultural soil (Costantini *et al*., 2009).

71 Redox reactions affect pedogenetic processes and reflect hydrological functioning
72 in the landscape. Even if landscape position is a consistent indicator of hydric soil in
73 wetlands, wetland soil in semiarid regions is problematic and has been studied much
74 less than those of humid regions. Semiarid wetlands undergo strong fluctuations of the
75 water table because of the irregular rain and are frequently saline (3–50 g l^{-1}) or
76 hypersaline (> 50 g l^{-1}) (Williams, 2002; Castañeda & Herrero, 2008). The dearth of
77 inventories of saline wetlands, and maps of soil and vegetation, hampers the
78 understanding of their ecological functions and hydric behavior. The limited amount of
79 available information results in little regulatory recognition and in wetland degradation
80 (Williams, 2002; Castañeda & Herrero, 2008). There has been little research on the
81 processes of oxidation and reduction in the soil of saline wetlands although the factors
82 that control the interactive effects of salinity and oxidation and reduction of iron under
83 laboratory (Cameron *et al*., 1984; King & Garey, 1999) or field (Snyder *et al*., 2004)
84 conditions have been published.

85 Relict redoximorphic features may be preserved in soil that was previously
86 saturated and reduced. Moreover, the development of redox features is only indirectly
87 related to how long soil has been saturated. Therefore, in the absence of site-specific

88 data on water table levels in Gallocanta Lake, we required a method that reflects the
89 current reducing conditions in the soil. Our aims were to identify the reducing
90 conditions of soil that are currently subjected to intermittent flooding in Gallocanta
91 Lake, to relate the degree of reduction to soil characteristics and to test the applicability
92 of IRIS tubes as a strategy for recognizing hydric soil in such semiarid conditions.
93
94 **Study area**
95 Gallocanta Lake, NE Spain, is the largest and best preserved saline lake in Western
96 Europe. It has been included in the Ramsar list since 1994 and is protected under the
97 European Union (EU) Birds and Habitats Directives. The lake is in a Quaternary
98 depression at the bottom of a karst polje within the Iberian Range at 1000 m a.s.l.
99 (Figure 1). The underlying Triassic lutites and interbedded evaporites contribute both to
100 the high salinity of the lake, which is characterized by alternating wet and dry periods,
101 and also to the subsequent variation in soil salinity (Castañeda *et al*., 2015) and water
102 chemistry (Comín *et al*., 1983).
103 The climate is dry semiarid with very irregular rainfall. The mean annual
104 precipitation for the last 70 years is 488 mm yr^{-1}; it ranges from 761 mm (in 1959) to
105 232 mm (in 2001). Mean temperature is 11.4 °C for the period 1969–2015, with 111
106 frost days per year. The mean annual water deficit is 605 mm (García-Vera & Martínez-
107 Cob, 2004) which is exacerbated by the frequent winds. The soil temperature regime is
108 mesic, and the soil moisture regime is generally aquic at the lake shore and xeric in
109 agricultural areas (Soil Survey Staff, 2014).
110 Water level fluctuation has received much attention, mainly because it can be used
111 to identify Quaternary climatic and environmental changes (Schütt, 1998). As compiled
112 by Luna *et al*. (2016), the highest water level was registered in 1974 at 2.84-m depth,

113 whereas during periods of low rainfall, which have been common in the last few
114 decades, all of the free water of the lake has evaporated.
115
116 **Methodology**
117 *Selection of sites*
118 We designed a purposive sampling scheme to detect redox conditions around the lake.
119 We selected sites that flood intermittently based on a review of historical aerial
120 photographs and Landsat images, geomorphic and pedological evidence (Castañeda *et*
121 *al*., 2015), and our field work that extended from 2009 to the present. Our selection
122 criteria required that the sites be undisturbed and accessible. At the time of the survey
123 most sites were dry. Historic photographs and satellite images provide a glimpse of the
124 conditions of the sites through time. The study sites were in different geomorphic units
125 which include lacustrine terraces, lake bed and silt–sand barriers (Figure 1 and Table 1).
126
127 *Installation and retrieval of the IRIS tubes*
128 The IRIS tubes used to document the development of reducing conditions in soil are
129 coated with an iron oxide suspension and the coating is dried afterwards (Castenson &
130 Rabenhorst, 2006; Jenkinson & Franzmeier, 2006). Under water saturated, anaerobic
131 and chemically reduced conditions, this coating is reduced by heterotrophic microbes
132 and then solubilized and stripped from the tubes.
133 Five or three IRIS tubes have been used as replicates (Rabenhorst, 2008; Dorau *et*
134 *al*. 2016, respectively) to account for soil heterogeneity. Sets of five IRIS tubes 60-cm
135 long with the lower 50 cm coated were installed at each site (Figure 1) between April
136 and July 2014. Five tubes were arranged in a cluster pattern within a one square metre
137 area following the procedure of Rabenhorst (2008). The tubes were inserted into auger

holes made in the soil with a 22-mm push probe. Instead of the four-week period used for basic monitoring with IRIS tubes (Rabenhorst, 2008), we left the tubes in place for between 22 and 34 weeks (Table 1). The removal of iron oxide was monitored every four weeks. This was done by examining the central tube (carefully removed and gently reinserted to avoid abrasion) of all sets for visual evidence of removal of the iron oxide coating. We retrieved the tubes in January 2015, except the set at site 5, which was retrieved in March when the surface water evaporated and the site was easily reached. Each tube was washed gently in the field with tap water to remove any soil that adhered, and then the tube was photographed three times with the tube rotated 120º between each. Photography was done in the field to record the black mottles of iron monosulphide (FeS) coating (Rabenhorst *et al*., 2010; Dorau *et al*., 2016) which are metastable minerals under aerated conditions.

The tubes were also y photographed systematically in the laboratory under vertical view with a fixed field of vision. The three photos of each tube were cropped and combined into a single digital image of the whole surface of the tube, and their cylindrical shape was projected into an equivalent plane. Black mottles on the IRIS tubes were quantified from the field photographs. The removal of iron oxide coating (Rabenhorst & Burch, 2006) was quantified for each binary image that was converted digitally. For each IRIS tube, the area of maximum removal of the iron oxide coating was calculated within the upper 30 cm of the tube, for a zone of 15 cm (Rabenhorst, 2008).

Laboratory analysis

The soil was sampled by auger (7 cm in diameter), except at sites 4 and 5 whose profiles were sampled and described in pits following Schoeneberger *et al*. (2012). Soil

163 samples were air-dried at room temperature before placing in an oven at ≤ 40 °C, and
164 sieved through a 2-mm mesh. Soil salinity was measured as the electrical conductivity
165 of the 1:5 soil:water extract (EC1:5) and the saturated paste extract (ECe). Electrical
166 conductivities were expressed in dS m^{-1} at 25 °C. Calcium carbonate equivalent (CCE)
167 was determined by the Bernard calcimeter method based on the reaction with HCl,
168 gypsum content was quantified by thermogravimetric analysis (Artieda *et al*., 2006) and
169 organic matter (OM) was quantified by chromic-acid digestion (Heanes, 1984) and a
170 UV/V UNICAM 8625 (Unicam Instruments Ltd., Cambridge, UK) spectrophotometer.
171 Particle-size distribution was assessed by laser diffraction (Malvern MASTERSIZER
172 2000, Malver, UK). The pH and EC of groundwater samples were measured with a pH
173 electrode and a conductivity cell (Orion 9157BNMD and Orion 013605MD,
174 respectively, Thermo Fisher Scientific Inc., Beverly, US) and major ions were
175 determined by ion chromatography (Metrohm 861 Advanced compact IC, Metrohm
176 AG, Herisau, Switzerland).

177 Surface soil samples (0–10 cm) at sites 4 and 5 that appeared black and smelled of
178 sulphur were incubated in the laboratory under aerobic conditions for 18 weeks, and pH
179 was measured weekly following the method of Creeper *et al*. (2012) and Grealish *et al*.
180 (2010). Undisturbed blocks of soil from selected horizons were impregnated with a
181 cold-setting polyester resin, and thin sections (135 mm × 58 mm and 58 mm × 42 mm)
182 were prepared by the method of Guilloré (1985) and described under polarizing
183 microscope following Stoops (2003).

184

185 **Results**

186 *Rainfall data during the survey*

187 Based on annual rainfall and following the criteria of the Soil Survey Staff (2014), the
188 year 2014 and years immediately preceding it would be considered to be 'normal'
189 precipitation years. The rainfall registered in 2014 at the lake border in Picos weather
190 station (Figure 1) was 377 mm, 23% less than the long-term mean of 488 mm. The
191 meteorological conditions during the study were characterized by a dry spring, with
192 only 53.7 mm of rain from March to May. The autumn was more humid than spring,
193 with 110 mm of rain from September to November. Observations of the depth of the
194 water table indicated that it dropped during spring and summer of 2014, and it did not
195 return to within 50 cm of the soil surface. The low spring rainfall together with the
196 dryness (low level) of the lake caused a delay in the extraction of the tubes until after
197 the autumn.
198
199 *Main soil features*
200 The soil is strongly saline (Table 2), with an ECe up to four times the salinity of the
201 ocean water (182 dS m^{-1}), and has a large CCE content that ranges from 18 to 70%. Soil
202 pH is mostly in the range between 7.6 and 8.6 and is probably dominated by of the large
203 CCE content. There is little organic matter in the soil of the lake fringes, < 2%, whereas
204 it reaches 6.2 and 5.8%, at the lake bottom (site 5) and where there are saline grasses
205 (site 1), respectively. The particle-size distribution indicates that soil texture is
206 essentially clay loam and sand content decreases with depth. Occasionally, gravels
207 accumulate in surface and subsurface horizons in areas where fluvial water enters the
208 lacustrine system (site 3).
209 The available descriptions of soil morphology in the area (Castañeda *et al*., 2015;
210 Luna *et al*., 2016) indicate waterlogging or restricted drainage, with Gypsic Aquisalids
211 at the lake bottom (Figure 2), Typic Aquisalids at the shoreline and Typic Calcixerepts

212 in slightly elevated areas (Table 1). The soil at the lowest topographic positions (sites 4
213 and 5) is a hydric soil that conforms to the field indicator requirements established by
214 USDA–NRCS (2010). At site 4, two horizons (Ag and 2Cg1) have a field indicator F3,
215 'depleted matrix' (USDA–NRCS, 2010), with a grey matrix colour (2.5Y and chroma ≤
216 2), and common redox mottles (7.5YR and 10YR, Table 2). At site 5, the profile has a
217 gleyed and an iron-depleted matrix with bluish, low chroma matrix colours (10B and
218 2.5GY and chroma < 2, Table 2), consistent with the field indicator F2, 'gleyed matrix'
219 (USDA–NRCS, 2010). Redox depletions (5Y and 10B) are abundant and are mainly
220 associated with the occurrence of gypsum layers.

221 Micromorphic pedofeatures related to redox processes in soil on the lake floor
222 include impregnated redoximorphic features such as banded iron and manganese oxide
223 hypocoatings. Coatings adjacent to voids occur in the soil of the surface horizon (Ayzg
224 horizon) where the abundance of biological remains favours the formation of a channel
225 to lenticular soil microstructure (Figure 2c). Accumulation of iron sulphides as
226 framboids, frequently clustered (Figure 2d), are common in subsurface horizons (Cyg3
227 horizon) with a massive to vughy microstructure and micritic cristalitic b-fabric as
228 defined by Stoops (2003).

229

230 *Groundwater characteristics*

231 On the dates that the IRIS tubes were installed, observed water table depth ranged from
232 –10 cm (site 1) to –100 cm (site 5) (Table 1). Free surface water occurred intermittently
233 at all sites during the study period. Groundwater is non-saline in the marsh (saline
234 grasses) and reed bed areas, sites 1 and 3. The current lake bed (sites 4 and 5) and the
235 SE terrace (site 2), show similar groundwater characteristics, with a pH of between 6.7
236 and 7.1 and high salinity (although with a two-fold difference in EC among the

237 unvegetated lakebed sites) with increased Mg^{2+} and $SO4^{2-}$ concentrations (Table 1).
238 Nitrates are more abundant in saline groundwater, in particular at sites 2 and 4. The
239 bicarbonate content is somewhat variable, with a 2- to 3-fold range between the
240 maximum (854 mg l^{-1}) at site 2 and the minimum (366 mg l^{-1}) at site 1.
241
242 *Iron oxide removal from the IRIS tubes*
243 The percentage area with depleted iron in a 15-cm zone within the upper 30 cm of the
244 tube for all five sites varies from 0.5 to 95.1%. It is also very variable between the five
245 tubes at a single site (Figure 3 and Table 3). The greatest variation in iron oxide removal
246 occurred at site 4 (standard deviation, SD, 39.7%), at the southern margin of the lake
247 (Figure 1 and Table 3). Variability at the other sites was more modest (SDs from 2.9%
248 to 11.5%). The zones of the tubes where the iron oxide coating was chemically reduced
249 and removed were almost lacking iron oxide in some cases, whereas in others these
250 zones retained a thin coating of iron oxide that contrasted distinctly from the original
251 reddish brown colour (Figure 3). Occasionally, zones depleted of iron occurred above
252 the zero level line, i.e. the mark on the tube that corresponded to 0 cm or ground-level.
253 The patterns of iron oxide removal included: (i) spots, corresponding to reducing
254 conditions at microsites, (ii) area of continuous removal, corresponding to the reducing
255 conditions in a whole horizon, 3) doughnut-shaped depletion patterns (Jenkinson &
256 Franzmeier, 2006) similar to that formed by bacterial cultures and (iv) linear depletion
257 patterns (Figure 3) often observed in areas with increased organic matter and microbial
258 activity (Vepraskas & Faulkner, 2001) related to the occurrence of roots as a source of
259 organic matter (Jenkinson & Franzmeier, 2006) because of the activity of
260 phytosiderosphores (Dorau *et al*., 2016).

The soil in sites 3 and 5 (Figure 4) can be classed as a hydric soil based on the degree of reduction, Technical Standard (NTCHS). A minimum of three out of five IRIS tubes have > 30% of their coating removed in a zone 15-cm long starting within 15 cm of the soil surface (Table 3). The rate of reduction, determined as the percentage of iron oxide depleted per month on the surface of the tube, ranges from 0.4 at site 1 (Ojos, Figure 1) to 12% at the neighbouring site 3 (Reguera).

Iron monosulphides can form as black mottles on IRIS tubes by the rapid chemical reaction of soluble sulphide with the iron oxide coatings (Rabenhorst *et al*., 2010). The black FeS mottles were especially intense at sites 2 and 5, with a mean of 1.4 and 5%, respectively (Table 3). Speciation of aqueous sulphide is pH dependent, and the alkaline pH of the calcareous soil (Table 2) suggests that the pore water sulphide is primarily present as hydrogen suphide (HS^-) (Garrels & Christ, 1965). Maximum percentage of black mottles per tube occurs at site 5, with a 12.2% cover of the whole tube (Table 3) and 19.2% of the upper 30 cm of the tube. It is likely that these represent minimum sulphide values for the tubes from site 5, because the black sulphide initially forms as a coating over the iron oxide coating (which strongly adheres to the tubing). However, if all of the iron oxide on the tube becomes converted to the black FeS (from large sulphide concentrations or over long periods of time), the FeS (without an undercoating of iron oxide) does not adhere to the tube and leaving the white tube exposed. Some parts of the white areas at the bottom of the tubes from site 5 appear like this (mostly dark grey and white with little or no iron oxide), Figure 3.

Discussion

The wet saline soil of the Gallocanta saline lake, which is subjected to intermittent flooding, shows evidence of the mobilization of iron and manganese oxides in exposed

286 soil (Figure 2a) or even temporarily at the soil surface (Figure 2b). In spite of the subtle
287 topography of the area (from 0.3 to 2.2 m of height difference among sites) the
288 elevation appears to condition the degree of reduction expressed in the iron oxide
289 removal from the IRIS tubes. The average percentage of iron oxide removed from 15
290 cm generally increases from 3% to 81% as the elevation decreases even if the
291 groundwater depth when the tubes were installed increases (Table 1). The site 3 is an
292 exception, with 0.6 m of relative elevation increase and an average iron oxide removal
293 of 81% to 95%, probably due to the surface water inflow from the Reguera intermittent
294 stream into the lake, producing longer periods of soil saturation in this mouth zone. The
295 neighboring sites 1 and 3 represent the minimum and maximum intensity of iron
296 depletion, respectively. Both sites have saline soil and fresh groundwater (Table 1) and
297 their level of soil OM does not seem to condition the removal of iron from the IRIS
298 tubes. A high percentage of iron oxide coating removal also occurs at the soil of site 5,
299 which has a high OM content (up to 6.2%) and gypsum (21% as mean) and where NO_3^-
300 is completely removed from groundwater (Table 1) by reduction to N_2.

301 The vertical distribution of iron depleted zones along the tubes are not uniform
302 (Figure 3) and shows a great variety of patterns similar to that described by Jenkinson &
303 Franzmeier (2006) in very different types of soils from a diversity of locations. Even in
304 a single depleted area of the tubes Dorau *et al*. (2016) recognize gradients of reducing
305 soil conditions.

306 The redox micromorphic pedofeatures show a redox gradient with soil depth,
307 which accords with the overall pattern of iron oxide removal shown by field
308 photographs of the IRIS tubes. The iron and manganese oxides in the surface horizon
309 (Figure 2c) indicate alternating reducing–oxidizing conditions, which are favoured by
310 the abundant coarse material and the more aerated soil microstructure. In contrast, iron

311 sulphides only accumulate at depth (Figure 2d), which indicate that reducing conditions
312 predominate because of the finer microstructure that controls soil porosity. Iron
313 hypocoatings can be produced after several days of water saturation, whereas the
314 formation of iron sulphides (pyrite) indicates very wet and reducing conditions from
315 several months of water saturation (Lindbo *et al*., 2010).

316 Contemporary or relict micromorphological features may occur in the same
317 horizon (Lindbo *et al*., 2010), but because of tubes had been installed for several months
318 we recorded features that are actively forming. Based on the redox sequence
319 (Ponnamperuma, 1972) and their corresponding E_H values summarized by Dorau &
320 Mansfeldt (2015), all the sites studied have at least moderate reducing soil conditions
321 because exhibit iron oxide removal which indicates E_H ranges from 100 to –100 mV.
322 Sulphate reduction and FeS deposition > 0.2% at sites 2, 3 and 5 indicate that these sites
323 have strongly reducing soil conditions with E_H values < –100 mV, especially site 5,
324 which is at the lowest landscape position where iron sulphide deposits were maximum.
325 According to the categories proposed by Bartlett & James (1995), soil at sites 2, 3 and 5
326 has a sulphidic redox status.

327 In contrast with other carbonate-rich environments (Stiles *et al*., 2010) and
328 laboratory observations (Couto *et al*, 1985), in Gallocanta Lake the expression of redox
329 features is not inhibited by the buffering capacity associated with the high content of
330 CCE (47% as mean). Additionally, in contrast observations in other soils (Craft, 2001)
331 the availability of NO_3^- in groundwater does not appear to hamper iron reduction and
332 mobilization in these soils. It is likely, however, that these components may reduce the
333 rate of development and expression of redox features.

334 Although we observed minor reduction of iron oxide coatings after four weeks at
335 the lake floor (site 5), generally the time needed for tubes to show evidence of soil

336 reducing conditions among all sites surrounding Gallocanta Lake was 27 weeks on
337 average (Table 1), which was very long when compared with the time (days to weeks)
338 required in non-carbonatic environments (Jenkinson & Franzmaier, 2006; Dorau *et al*.,
339 2016) or in controlled experiments (Rabenhorst *et al*., 2008; Dorau & Mansfeldt, 2015).
340 The effect of carbonate content was observed during soil incubation, where, despite the
341 presence of oxidizable sulphide, the decrease in pH (down to 7.3 during the first two
342 weeks before rising to slightly alkaline values, 7.8) was inhibited in those soils which
343 had 17.4% and 37.6% of CCE (Table 2), similar to reports by Couto *et al*. (1985) under
344 controlled conditions. However, the seasonal inundation observed in Gallocanta Lake
345 suggests the occurrence of intermittent water saturation of soil, which is probably the
346 main reason of the low reduction rate found at our soil. Additionally, the delay in
347 reduction timeframes may also be affected by the high carbonate content. As already
348 demonstrated by Dorau & Mansfeldt (2015), the use of Mn-oxide coated tubes may
349 improve the IRIS method by the preferential reductive dissolution of manganese over
350 iron oxides, thus reducing the time of monitoring and enhancing the differences in
351 intensity of reduction between sites.

352 There is no clear relationship between soil or groundwater composition (and
353 salinity) and the degree of iron removal from IRIS tubes, despite an eight-fold range in
354 ECe (Table 2) and a 50-fold difference in groundwater salinity (Table 1). The bacterial
355 iron oxidation is completely inhibited with 3% (wt/vol) of NaCl ($\cong$ 40 dS m^{-1}) under
356 laboratory conditions (Cameron *et al*., 1984) whereas in the soil studied it occurs at
357 much higher salinity (Table 1) indicating the complexity of natural conditions. This
358 issue would require a fully experimental approach, i.e. controlled conditions only
359 achievable in laboratory or microcosm experiments. This is beyond the scope of this
360 paper.

361 The iron oxide coating removal is expected to occur mainly when the water table
362 is high. Although continuous water table data are not available for the IRIS sites during
363 the period of study, one can reasonably assume that the occurrence of shallow water
364 table caused the development of anaerobic conditions and the reduction of iron oxide
365 from the IRIS tubes at sites 3 and 5, and probably at site 4. As introduced by Dorau *et*
366 *al*. (2016), the monitoring of water tables in parallel to that of iron removal from IRIS
367 tubes would produce more meaningful data for normalizing the iron removal per unit of
368 time (day or week) when water tables are near (within 30 cm of) the soil surface.
369 However, the intensity and duration of reducing soil conditions should be considered as
370 conditioned by multiple factors, and not only by the water table depth or other single
371 soil parameter. The organic matter type and content, pH, soil temperature, and microbial
372 community can vary between sites, making difficult to predict or normalize iron
373 removal, even within a wetland.
374
375 **Conclusions**
376 This study demonstrates that IRIS tubes are of value to document the development of
377 reducing conditions in saline and carbonate-rich wet soil from research at Gallocanta
378 Lake where the water level fluctuates seasonally and annually. The identification of
379 current reduction in the soil of different geomorphic and edaphic units around the lake
380 confirms that previously observed macro and micromorphological redoximorphic
381 features are probably developing at present in spite of the intermittent dryness of the
382 lake. The alkaline conditions with waterlogging grant novelty to our work.
383 The differences in magnitude of iron oxide depletion from the IRIS tubes between
384 sites show little association with soil composition or salinity, but seem to be related
385 mainly to subtle differences in topography that control when the soil becomes saturated

386 and reducing conditions persist. Interpretation of the processes and factors responsible
387 for the differences in the amount and patterns of iron depletion from the IRIS tubes
388 between sites remain unsolved. This critical limitation of our field approach also poses a
389 subject for future research which should be complemented with laboratory or
390 microcosm experiments.
391
392 **Acknowledgements**
393 This work is a result of the research projects PCIN–2014–106, funded by the Spanish
394 Government, and I–COOP–2016SU0015, funded by the Spanish National Research
395 Council (CSIC). We acknowledge the data provided by the Spanish Meteorological
396 Agency (AEMET) after contract no L2 990130734. E. Luna was financed by a
397 fellowship from the Aragón Government, Spain. Two anonymous reviewers and the
398 Editor helped to improve the paper.
399
400 **References**
401 Artieda, O., Herrero, J. & Drohan, P.J. 2006. A refinement of the differential water loss
402 method for gypsum determination in soils. *Soil Science Society of America Journal*,
403 **70,** 19321935.
404 Bartlett, R.J. & James, B.R. 1995. System for categorizing soil redox status by chemical
405 field testing. *Geoderma*, **68,** 211–218.
406 Cameron, F.J. Jones, M.V. & Edwards, C. 1984. Effects of salinity on bacterial iron
407 oxidation. *Current Microbiology*, **10,** 353–356.
408 Castañeda, C. & Herrero, J. 2008. Assessing the degradation of saline wetlands in an
409 arid agricultural region in Spain. *Catena*, **72,** 205–213.

410 Castañeda, C., Gracia, F.J., Luna, E. & Rodríguez-Ochoa, R. 2015. Edaphic and
411 geomorphic evidences of water level fluctuations in Gallocanta Lake, NE Spain.
412 *Geoderma*, **239–240,** 26–279.
413 Castenson, K.L. & Rabenhorst, M.C. 2006. Indicator of reduction in soil (IRIS):
414 Evaluation of a new approach for assessing reduced conditions in soil. *Soil Science*
415 *Society of America Journal*, **70,** 1222–1226.
416 Comín, F., Alonso, M., Lopez, P. & Comelles, M. 1983. Limnology of Gallocanta Lake,
417 Aragon, northeastern Spain. *Hydrobiologia*, **105,** 207–221.
418 Costantini, E.A.C., Pellegrini, S., Bucelli, P., Storchi, P., Vignozzi, N., Barbetti, R. &
419 Campagnolo, S. 2009. Relevance of the Lin's and Host hydropedological models to
420 predict grape yield and wine quality. *Hydrology and Earth System Sciences*, **13,**
421 1635–1648.
422 Couto, W., Sanzonowicz, C. & Barcellos, A. de O. 1985. Factors affecting oxidation-
423 reduction processes in an Oxisol with a seasonal water table. *Soil Science Society of*
424 *America Journal*, **49,** 1245–1248.
425 Craft, C.B. 2001. Biology of wetland soils. In: *Wetland Soils: Genesis, Hydrology,*
426 *Landscapes, and Classification* (eds J.L. Richardson & M.J. Vepraskas), pp. 107–
427 135. CRC Press, LLC, Boca Raton, FL.
428 Creeper, N., Fitzpatrick, R. & Shand, P. 2012. A simplified incubation method using
429 chip-trays as incubation vessels to identify sulphidic materials in acid sulphate
430 soils. *Soil Use Management*, **28,** 401–408.
431 Dorau, K. & Mansfeldt, T. 2015. Manganese-oxide-coated redox bars as an indicator of
432 reducing conditions in soils. *Journal of Environmental Quality*, **44,** 696–703.

433 Dorau, K., Eickmeier, M. & Mansfeldt, T. 2016. Comparison of manganese and iron
434 oxide-coated redox bars for characterization of the redox status in wetland soils.
435 *Wetlands*, **36,** 133–141.
436 García-Vera, M.A. & Martínez-Cob, A. 2004. Evolución del contenido de humedad y
437 de la tasa de evaporación en humedales: aplicación a la Laguna de Gallocanta.
438 2004-PH-14-I, Zaragoza, Spain (In Spanish). URL http://hdl.handle.net/10261/2976
439 [accessed on 15 Nov 2016].
440 Garrels, R.M. & Christ, C.L. 1965. *Solutions, Minerals, and Equilibria*. Harper and
441 Row, New York, NY.
442 Grealish, G., Fitzpatrick, R. & Shand, P. 2010. Acid sulphate soil toposequences in
443 wetlands of the Lower River Murray. In: *Soil Solutions for a Changing World,*
444 Proceedings of the 19th Congress of Soil Science, pp 17–20, 1–6 August, Brisbane,
445 Australia. Published on DVD.
446 Guilloré, P. 1985. *Méthode de Fabrication Mécanique et en Série des Lames Minces*,
447 3rd edn, Institut National Agronomique, Paris-Grignon, France (In French).
448 Heanes, D.L. 1984. Determination of total organic-C in soils by an improved chromic
449 acid digestion and spectrophotometric procedure. *Communications in Soil Science*
450 *and Plant Analysis*, **15**, 1191–1213.
451 IUSSWorking Group WRB 2015. *World Reference Base for Soil Resources 2014.*
452 *International Soil Classification System for Naming Soils and Creating Legends for*
453 *Soil Maps*. World Soil Resources Report No 106, FAO, Rome, Italy.
454 Jenkinson, B.J. & Franzmeier, D.P. 2006. Development and evaluation of Iron–coated
455 tubes that indicate reduction in soils. *Soil Science Society of America Journal*, **70,**
456 183–191.

457 King, G.M. & Garey, M.A. 1999. Ferric Iron reduction by bacteria associated with the
458 roots of freshwater and marine macrophytes. *Applied and Environmental*
459 *Microbiology*, **65,** 4393–4398.
460 Luna, E., Castañeda, C., Gracia, F.J. & Rodríguez-Ochoa, R. 2016. Late Quaternary
461 pedogenesis of lacustrine terraces in Gallocanta Lake, NE Spain. *Catena*, **147,** 372–
462 385.
463 Lindbo, D.L., Stolt, M.H. & Vepraskas, M.J. 2010. Redoximorphic features. In:
464 *Interpretation of Micromorphological Features of Soils and Regoliths. Their*
465 *Relevance for Pedogenic Studies and Classifications* (eds G. Stoops, V. Marcelino
466 & F. Mees), pp. 129–147, Elsevier, Oxford, UK.
467 Ponnamperuma, F.N. 1972. The chemistry of submerged soils. *Advances in Agronomy*,
468 **24,** 29–96.
469 Rabenhorst, M.C. 2008. Protocol for using and interpreting IRIS tubes. *Soil Survey*
470 *Horizons*, **49**, 74–77.
471 Rabenhorst, M.C. 2012. Simple and reliable approach for quantifying IRIS tube data.
472 *Soil Science Society of America Journal*, **76**, 307-308.
473 Rabenhorst, M.C. & Burch, S.N. 2006. Synthetic iron oxides as an indicator of
474 reduction in soils (IRIS). *Soil Science Society of America Journal*, **70,** 1227–1236.
475 Rabenhorst, M.C., Bourgault, R.R. & James, B.R. 2008. Iron oxyhydroxide reduction in
476 simulated wetland soils: Effects of mineralogical composition of IRIS paints. *Soil*
477 *Science Society of America Journal*, **72,** 1838–1842.
478 Rabenhorst, M.C., Megonigal, J.P. & Keller, J. 2010. Synthetic iron oxides for
479 documenting sulphide in marsh pore water. *Soil Science Society of America*
480 *Journal*, **74,** 1383–1388.

481 Rodó, X., Giralt, S., Burjachs, F., Comín, F., Tenorio, R.G. & Julià, R. 2002. High-
482 resolution saline lake sediments as enhanced tools for relating proxy paleolake
483 records to recent climatic data series. *Sedimentary Geology*, **148,** 203–220.
484 Schoeneberger, P.J., Wysocki, D.A., Benham, E.C. & Soil Survey Staff. 2012. *Field*
485 *Book for Describing and Sampling Soils,* Version 3.0. Natural Resources
486 Conservation Service, National Soil Survey Center, Lincoln, NE.
487 Schütt, B. 1998. Reconstruction of Holocene paleoenvironments in the endorheic basin
488 of Laguna de Gallocanta, Central Spain by investigation of mineralogical and
489 geochemical characters from lacustrine sediments. *Journal of Paleolimnology*, **20,**
490 217–234.
491 Snyder, M., Taillefert, M. & Ruppel. C. 2004. Redox zonation at the saline-influenced
492 boundaries of a permeable surficial aquifer: Effects of physical forcing on the
493 biogeochemical cycling of iron and manganese. *Journal of Hydrology*. **296,** 164–
494 178.
495 Soil Survey Staff. 2014. *Keys to Soil Taxonomy*, 12th edn,. U.S. Department of
496 Agriculture, Natural Resources Conservation Service, Washington, DC.
497 Stiles, C.A., Dunkinson, E.T., Ping, C.L. & Kidd, J. 2010. Initial field installation of
498 manganese indicators of reduction in soils, Brooks Range, AK. *Soil Survey*
499 *Horizons*, **51,** 102–107.
500 Stoops, G. 2003. *Guidelines for Analysis and Description of Soil and Regolith Thin*
501 *Sections*. Soil. Science Society of America, Inc., Madison, WI.
502 USDA-NRCS. 2010. *Field Indicators of Hydric soils in the United States*, version 7.0
503 (eds L.M. Vasilas, G.W. Hurt & C.V. Noble). USDA, NRCS, in cooperation with
504 the National Technical Committee for Hydric Soils. Washington, DC.

505 Veneman, P.L.M., Vepraskas, M.J. & Bouma, J. 1976. The physical significance of soil
506 mottling in a Wisconsin toposequence. *Geoderma*, **15,** 103–118.
507 Vepraskas, M.J. & Faulkner, S.P. 2001. Redox chemistry of hydric soils. In: *Wetland*
508 *Soils: Genesis, Hydrology, Landscapes, and Classification* (eds J.L. Richardson &
509 M.J. Vepraskas), pp. 85–106. CRC Press, LLC, Boca Raton, FL.
510 Williams, W.D. 2002. Environmental threats to salt lakes and the likely status of inland
511 saline ecosystems in 2025. *Environmental Conservation*, **29,** 154–167.
512

513 **Figure captions**

514 **Figure 1** Colour-shaded LiDAR-derived digital elevation model of Gallocanta Lake
515 with major contour lines and locations of the IRIS tubes.

516 **Figure 2** Evidence of iron and manganese mobilisation in Gallocanta Lake: (a) in
517 recently exposed soil at site 4, (b) at the soil surface in nearby areas subjected to
518 intermittent flooding. Thin sections show redox micromorphic pedofeatures
519 associated with voids (v), (c) manganese oxide (Mn) and iron-manganese oxide
520 (Fe/Mn) impregnated hypocoatings observed with plane polarized light, Ayzg and
521 (d) framboidal iron sulphide (FeS) coating observed with oblique incident light,
522 2Cyg3.

523 **Figure 3** Photographs taken in the field of five replicate IRIS tubes from each site when
524 they were extracted at the completion of the study.

525 **Figure 4** Photographs of IRIS tubes taken in the laboratory which show the upper 30
526 cm of the tubes. Black areas correspond to the iron oxide coating removed and red
527 boxes indicate the 15-cm section of the 30-cm tube with maximum removal of iron
528 oxide coating.

529

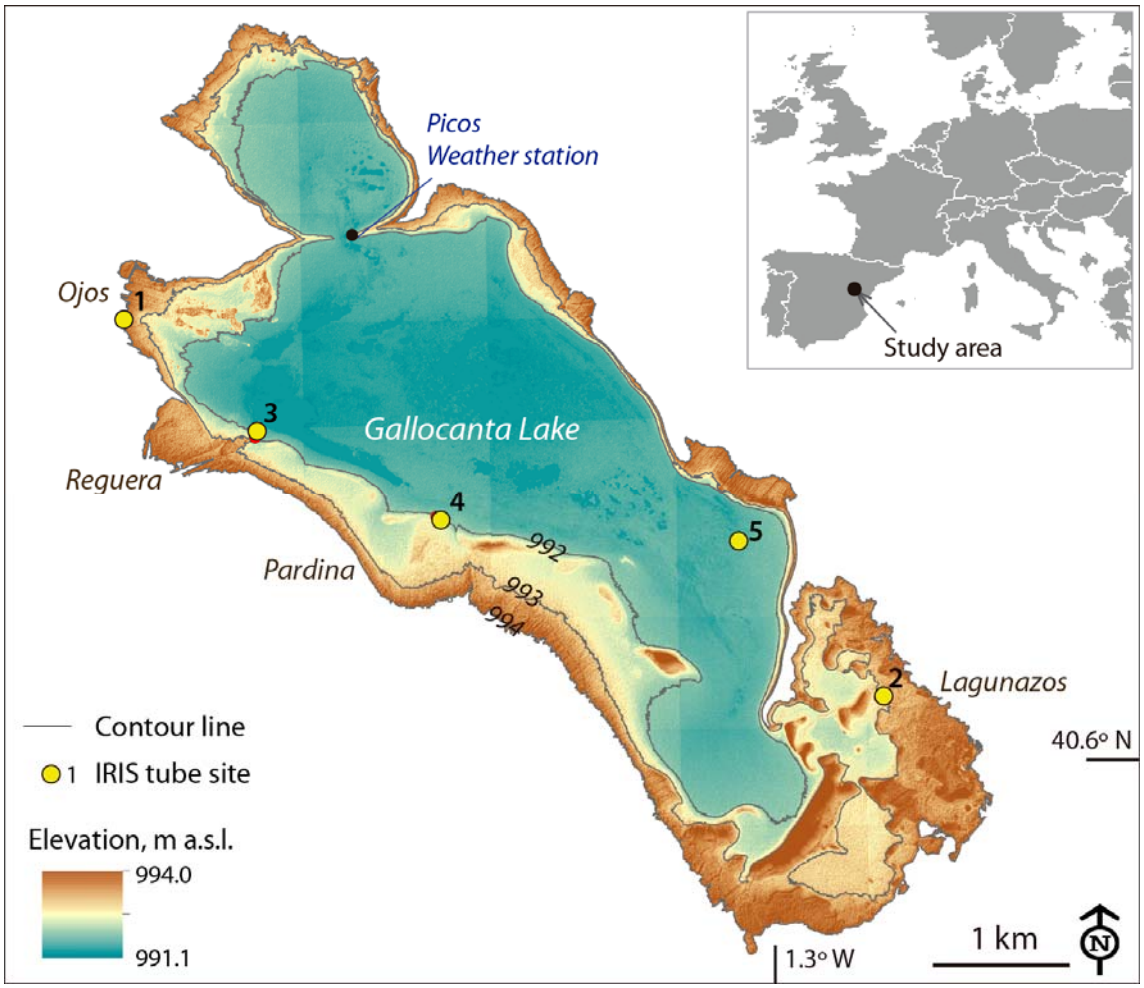
Picos
Weather station
Ojos
1
3
Gallocanta Lake
Reguera
4
5
992
993
994
Pardina
2
Lagunazos
Study area
Contour line
1 IRIS tube site
Elevation, m a.s.l.
994.0
991.1
40.6° N
1.3° W
1 km
N

530

531

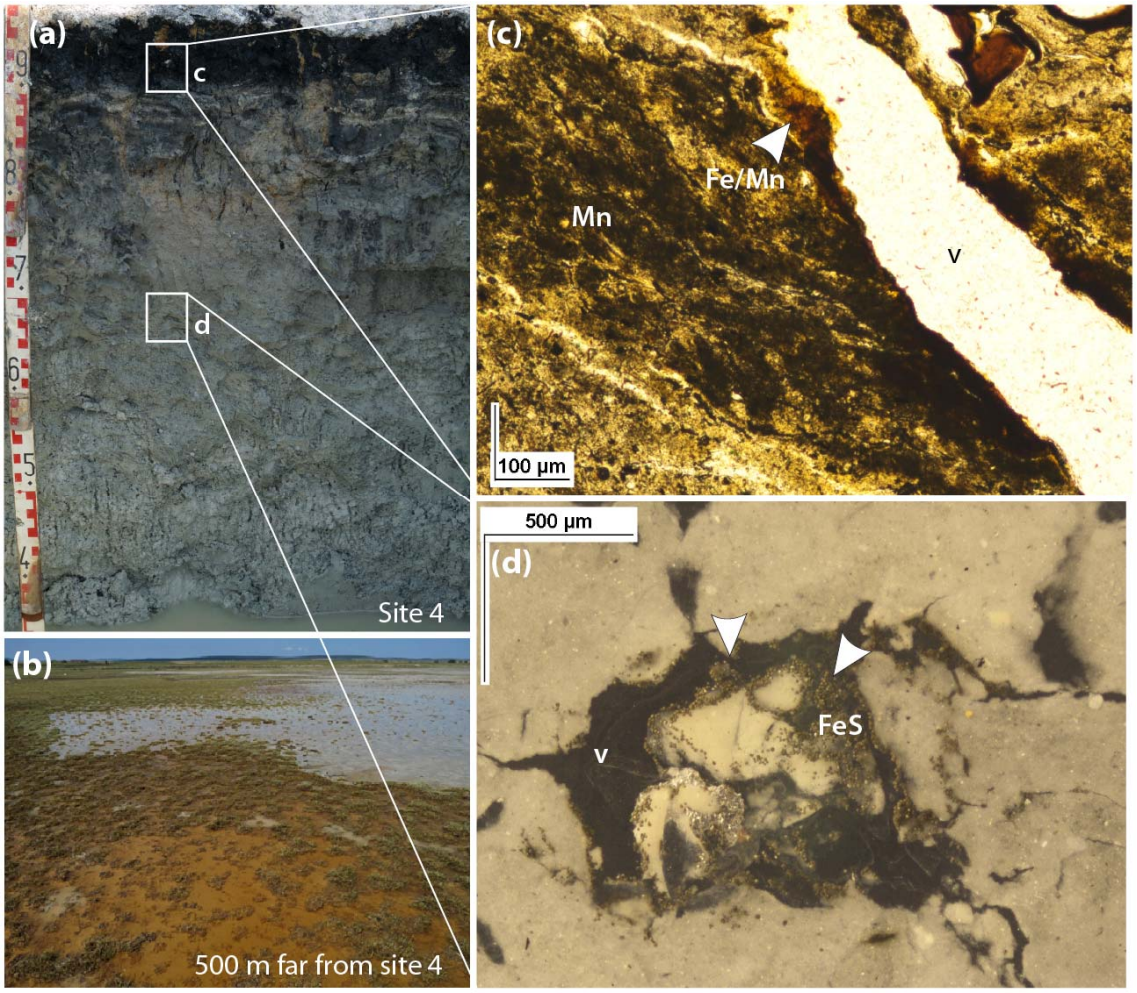

532

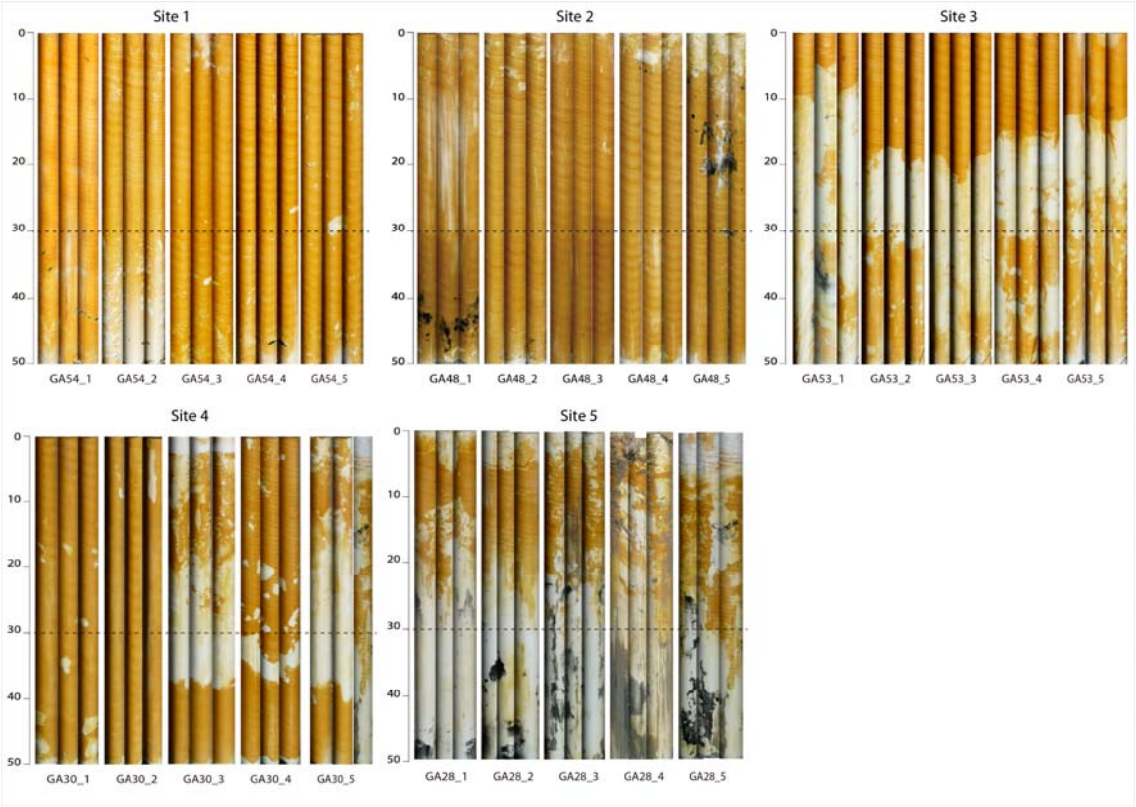
Site 1
Site 2
Site 3
Site 4
Site 5
GA54_1
GA54_2
GA54_3
GA54_4
GA54_5
GA48_1
GA48_2
GA48_3
GA48_4
GA48_5
GA53_1
GA53_2
GA53_3
GA53_4
GA53_5
GA30_1
GA30_2
GA30_3
GA30_4
GA30_5
GA28_1
GA28_2
GA28_3
GA28_4
GA28_5

533

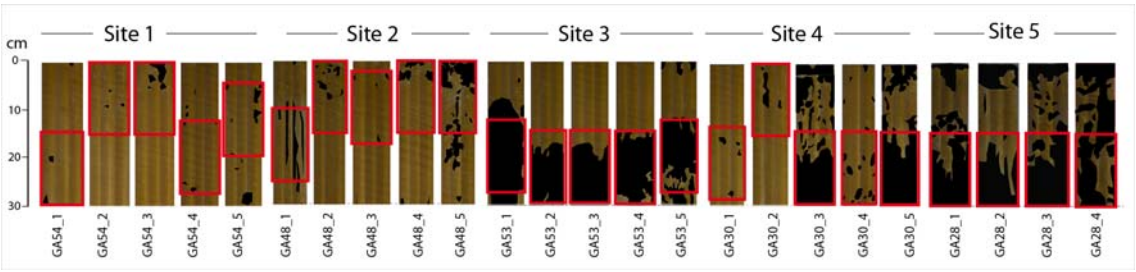
cm
Site 1
Site 2
Site 3
Site 4
Site 5
GA54_1
GA54_2
GA54_3
GA54_4
GA54_5
GA48_1
GA48_2
GA48_3
GA48_4
GA48_5
GA53_1
GA53_2
GA53_3
GA53_4
GA53_5
GA30_1
GA30_2
GA30_3
GA30_4
GA30_5
GA28_1
GA28_2
GA28_3
GA28_4

534

Table 1 Selected characteristics of sampled sites and groundwater

Site	Reference name	Elevation / m a.s.l.	Geomorphic unit	Soil classification		Landcover	Total number of weeks	Ground water depth	pH	EC[c]	NO_3^{-}[d]	SO_4^{2-}	$HCO3^{-}$	NH_4^{+}	Mg^{2+}
				ST[a]	WRB[b]			/cm		/dS m^{-1}	———	———	/mg l^{-1}	———	———
1	GA54	994.0	NW lacustrine terrace	ND		Saline grasses	22	–10	8.1	2.21	0.436	442	366	0.358	158
2	GA48	992.8	SE lacustrine terrace	Typic Calcixerept	Haplic Calcisol	Rush salt marshes	34	–23	6.9	17.5	19.4	5487	854	1.97	1295
3	GA53	992.4	Submerged silt–sand deposit	ND		Reed formations	22	–27	8.2	1.97	0.286	216	610	0.440	99.4
4	GA30	992.1	Sandy barrier	Typic Aquisalid	Gleyic Solonchak	Bare soil	30	–28	7.1	58.5	26.5	10 594	549	7.85	4893
5	GA28	991.8	Lake bed	Gypsic Aquisalid	Gypsic Gleyic Solonchak	Bare soil	30	–100	6.7	104	n.d.	29 408	488	20.6	11751

[a]USDA Soil Taxonomy (Soil Survey Staff, 2014). ND= not determined.
[b]World Reference Base (IUSS Working Group WRB, 2015).
[c]Electrical conductivity.
[d]n.d. = not detected.

Table 2 Main characteristics of the upper 50 cm of soil at the IRIS tubes sites

Depth /cm	Horizon	Munsell colour (Moist) Matrix	Mottles	pH 1:2.5	pH paste	EC1:5[a]	ECe[b]	CCE[c]	Gypsum	OM[d]	Gravels	Sand	Silt	Clay	USDA textural class
						— /dS m^{-1} —					/%				
Site 1 (GA54), auger hole															
0–25				7.6		1.2	21.3	49.9	3.7	5.8	0.6	37.8	42.2	20.0	Loam
25–50				7.9		0.6	19.1	49.9	2.9	3.8	0.9	26.0	44.5	29.4	Clay loam
Site 2 (GA48), auger hole															
0–25				8.3		0.3	18.1	28.9	3.6	1.1	1.9	34.5	38.3	27.2	Clay loam
25–50				8.1		0.8	19.9	31.7	< 2.0	0.4	2.6	35.4	41.6	23.0	Loam
Site 3 (GA53), auger hole															
0–25				7.9		0.7	19.3	45.4	< 2.0	0.4	30.6	53.3	15.0	31.6	Sandy clay loam
25–50				8.0		0.6	19.1	45.1	< 2.0	0.4	23.5	34.7	29.8	35.5	Clay loam
Site 4 (Pedon GA30)															
0–10	Ag	2.5Y 6/2	7.5YR 6/6		8.3	9.4	67.7	37.6	4.4	0.8	0.8	61.2	18.5	20.4	Sandy clay loam
10–25	2Cg1	2.5Y 6.5/1.5	10YR 6/6		8.1	8.3	39.3	58.7	3.8	0.5		14.1	49.0	36.9	Silty clay loam
25–50	2Cg2	2.5Y 7/1.5			8.1	4.0	25.7	69.7	2.2	0.5		23.6	33.3	43.1	Clay
Site 5 (Pedon GA28)															
0–6/10	Ayzg	10B 2.5/1			7.9	65.8	182	18.4	27.1	5.8		79.8	15.5	4.7	Loamy sand
6/10-14/16	Cyg1	10B 2.5/1–5Y 6/1	5Y 6/1		8.5	36.2	146	29.3	14.5	6.2		62.4	25.1	12.4	Sandy loam
14/16–24	Cyg2	10B 5.5/1	10B 5.5/2		8.6	23.7	104	36.6	17.0	3.9		44.0	31.6	24.4	Loam
24–42	2Cyg3	2.5GY 6/1	10B 4.5/1		8.2	23.2	100	28.0	28.6	3.4		44.8	26.4	28.8	Clay loam
42-50	2Cyg4	7.5GY 6/1			7.9	22.6	97.5	52.0	5.7	1.2	0.8	15.0	40.2	44.7	Silty clay

[a]Electrical conductivity of the soil:water 1:5 extract.
[b]Electrical conductivity of the saturation extract; ECe for sites 1 to 4 was estimated by regression between EC1:5 and ECe of samples from GA28 and GA30 (Castañeda *et al*., 2015).
[c]Calcium carbonate equivalent.
[d]Organic matter.

Table 3 Percentage of iron oxide depleted from a 15-cm zone of the IRIS tubes within the upper 30 cm of the soil surface (the main zone of interest when considering hydric soil issues) and percentage of black FeS mottles deposited on the tube

Iron oxide removal on a 15-cm zone	Site 1	Site 2	Site 3	Site 4	Site 5
Number of IRIS tubes					
Total	5	5	5	5	4
With ≥ 30% iron oxide coating removal	0	1	5	2	4
Surface removal / %					
Mean	3.0	12.3	80.8	33.9	70.4
Median	1.5	8.2	75.8	8.9	69.6
Standard deviation	2.9	11.5	8.8	39.7	9.1
Maximum	7.1	30.4	95.1	86.8	80.9
Minimum	0.5	1.0	74.1	2.1	61.5
Range	6.6	29.4	21.0	84.7	19.4
Monthly rate	0.4	1.3	12.0	3.9	6.9
Percentage of black FeS mottles[a]					
T1	0.4	2.6	1.8	0.1	5.4
T2	0.4	0.2	0	0	0.4
T3	0	0.1	0	0	12.2
T4	0.2	0.2	0.2	0.2	2.3
T5	0.2	3.6	0.1	0.1	4.6
Mean(SD)	0.2(0.1)	1.4(1.7)	0.4(0.8)	0.1(0.1)	5.0(4.5)

[a]FeS mottles that occurred along the full 50-cm length of the IRIS tubes at the time they were extracted from the field; T, tube; SD, standard deviation.